

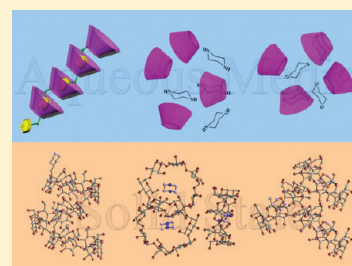
# Molecular Binding and Assembly Behavior of $\beta$ -Cyclodextrin with Piperazine and 1,4-Dioxane in Aqueous Solution and Solid State

Ying-Ming Zhang, Zi-Xin Yang, Yong Chen, Fei Ding, and Yu Liu\*

Department of Chemistry, State Key Laboratory of Elemento-Organic Chemistry, Nankai University, Tianjin 300071, People's Republic of China

## Supporting Information

**ABSTRACT:** The molecular binding behaviors of mono-[6-deoxy-6-(1-piperazinyl)]- $\beta$ -cyclodextrin (**1**), piperazine/ $\beta$ -cyclodextrin complex (**2**), and dioxane/ $\beta$ -cyclodextrin complex (**3**) were systematically investigated by NMR spectroscopy, mass spectrometry, dynamic light scattering, viscosity measurements, microcalorimetry, crystallography, and electron microscopic observations, displaying that the self-aggregation of piperazine-modified cyclodextrin **1** in both aqueous solution and the solid state produced a head-to-tail polymeric helical structure. In contrast, the cyclodextrin units in piperazine/ $\beta$ -cyclodextrin complex **2** were located in a staggered pattern, which was strikingly distinctive from the reported results by slow solvent evaporation method. Despite the fact that piperazinyl moiety was introduced by covalent and noncovalent chemical bonds in compound **1** and complex **2**, respectively, these two superstructures have the same crystal systems and space groups, which was clearly distinguished from the crystal structure of complex **3** and native  $\beta$ -cyclodextrin. These results indicated that the hydrogen bonding interconnection was a crucial and basic factor to govern the unique aggregation structures of supramolecular assemblies.



## INTRODUCTION

Molecular recognition and multicomponent assembly based on cyclodextrin (CD) derivatives is an essential part of supramolecular chemistry.<sup>1</sup> Possessing 6–8 D-glucose units linked by  $\alpha$ -1,4-glucose bonds, CDs can be functionalized to encapsulate various organic substrates in their hydrophobic microenvironments through the cooperative contribution of noncovalent forces,<sup>2</sup> including hydrophobic,  $\pi$ - $\pi$  stacking, van der Waals, and hydrogen bonding interactions. Subsequently, considerable effort has been devoted to exploring the structure–activity relationship of CD derivatives under distinct reaction conditions.<sup>3</sup> Among the numerous substituents and guest molecules that are available for the complexation with CDs, the ones with aromatic or bulky aliphatic moieties<sup>4</sup> have been intensively studied during the past several decades, due to their immense advantages to form the elaborated topological structures of self-included intramolecular complexes and self-excluded one-dimensional nanoarchitectures with biocompatible and electroactive properties.<sup>5</sup> For instance, Lincoln and co-workers designed a drug delivery system based on the modified CDs substituted with primary and secondary amines, in which these agents could be released in active form at specific sites.<sup>6</sup> Taking advantage of the isomerization of stilbene-modified  $\alpha$ -CD, Harada et al. constructed a photochemically controlled switch between double-threaded dimer and nonthreaded supramolecular self-assembly.<sup>7</sup> Recently, we successfully synthesized two  $\beta$ -CD analogues bearing azobenzene and triazole groups with the same composition but remarkably different conformations, revealing a self-locked bimolecular capsule and self-unlocked linear supramolecules, respectively.<sup>8</sup> Nevertheless, the comparative study on the conformational

changes of CDs toward structurally similar substrates through covalent and noncovalent chemical methods is still rare, to the best of our knowledge.

In the present work, we chose two molecular analogues, piperazine and 1,4-dioxane, to construct three well-defined crystal superstructures of mono-[6-deoxy-6-(1-piperazinyl)]- $\beta$ -CD (**1**), piperazine/ $\beta$ -CD complex (**2**), and dioxane/ $\beta$ -CD complex (**3**) by the method of slow solvent evaporation and hydrothermal synthesis, with the aim of comprehensive investigation of the critical factors to efficiently modulate the geometries of supramolecular assemblies in aqueous media and the solid state.

## RESULTS AND DISCUSSION

**Synthesis of Crystals 1–3.** The synthetic route of CD derivatives **1–3** is shown in Scheme 1. Mono-[6-deoxy-6-(1-piperazinyl)]- $\beta$ -CD (**1**) was synthesized by the reaction of mono-[6-*O*-(*p*-toluenesulfonyl)]- $\beta$ -CD and piperazine hexahydrate in a satisfactory field, which was fully characterized by <sup>1</sup>H NMR, <sup>13</sup>C NMR spectroscopy, ESI-MS, and elemental analysis (Figures S1–S3, Supporting Information). Then the saturated solution of **1** was allowed to slowly cool to room temperature, and colorless single crystals occurred after 2 weeks of slow solvent evaporation. The crystals of piperazine/ $\beta$ -CD (**2**) and dioxane/ $\beta$ -CD complex (**3**) were obtained in the presence of excess guest molecules under hydrothermal conditions for 2 days.

Received: November 1, 2011

Revised: December 21, 2011

Published: January 11, 2012

Scheme 1. Synthetic Routes of 1, 2, and 3

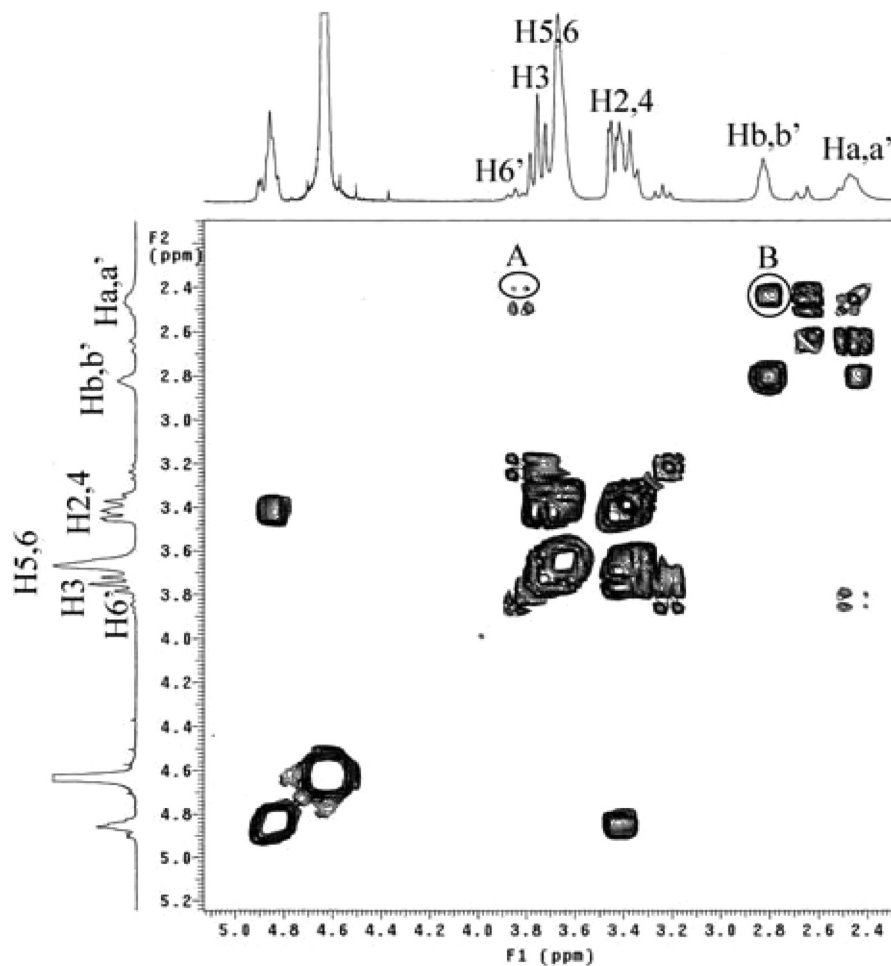
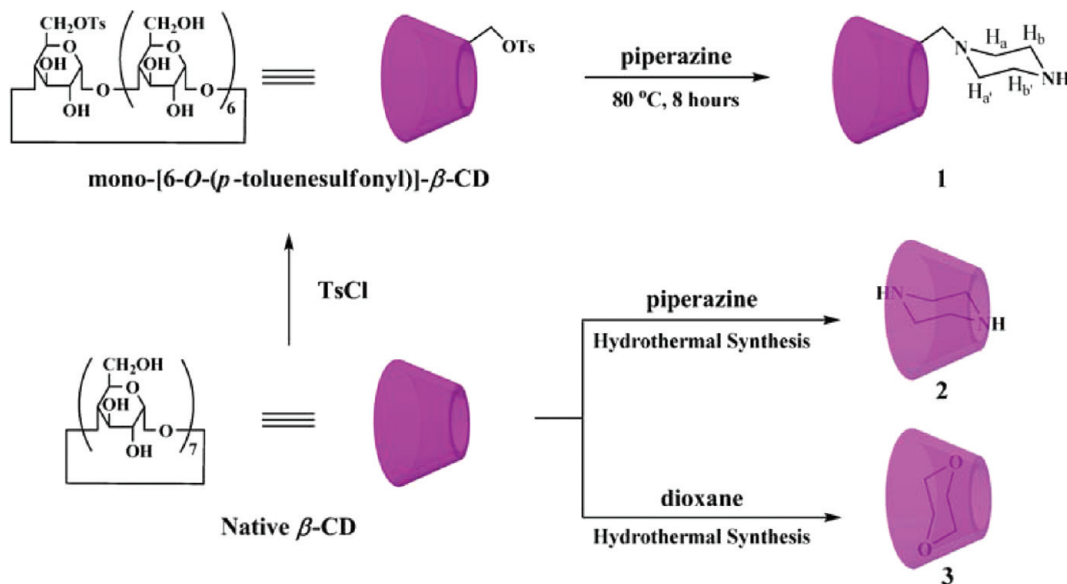


Figure 1.  $^1\text{H}$  COSY spectrum of **1** (2.28 mM, 300 MHz,  $\text{D}_2\text{O}$ , 25  $^\circ\text{C}$ ).

**Self-Assembly Behaviors of 1–3 in Solution.** First, the  $^1\text{H}$  resonances for the piperazine moiety of **1** were assigned by the use of 2D NMR correlation spectroscopy (COSY) recorded in  $\text{D}_2\text{O}$  (Figure 1), in which the CD signals correlated with a resonance at 2.41 ppm (peaks A), and in turn, this resonance

correlated with an isolated signal at 2.82 ppm (peaks B). The phenomena described above jointly assigned these two signals to the protons  $\text{H}_{\text{a,a}'}$  and  $\text{H}_{\text{b,b}'}$  of the adjacent methylenic group in the piperazine moiety as illustrated in Scheme 1. Furthermore, rotating-frame Overhauser effect spectroscopy

(ROESY) experiments were performed to obtain the structural information for **1** in aqueous solution, displaying clear nuclear Overhauser enhancement (NOE) cross-peaks between the  $H_{b,b'}$  protons of piperazine and the interior protons of  $\beta$ -CD cavity (peaks A in Figure S6, Supporting Information). These NOE cross-peaks indicated that the piperazinyl ring was accommodated in the hydrophobic cavity of  $\beta$ -CD.

Considering that dimerization is a key process to form highly ordered polymeric species,<sup>9</sup> the stability of aggregation in aqueous solution was quantitatively investigated. As shown in Figure 2,  $^1\text{H}$  NMR spectral changes of **1** were concentration

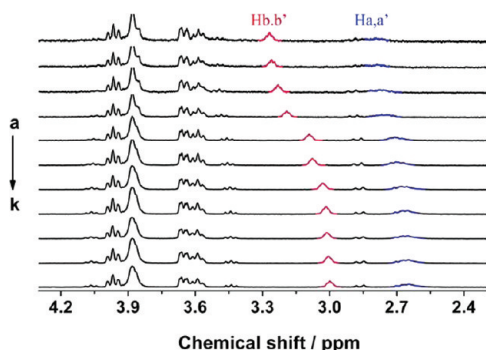


**Figure 2.**  $^1\text{H}$  NMR spectral changes of piperazinyl moiety of **1** ( $H_{a,a'}$  and  $H_{b,b'}$ ) in  $\text{D}_2\text{O}$  containing 0.5%  $\text{CH}_3\text{CN}$  as an internal standard at  $25^\circ\text{C}$  ( $[\text{1}] = 0.10, 0.12, 0.15, 0.20, 0.40, 0.50, 0.60, 0.95, 1.04, 1.16,$  and  $1.30$  mM from a to k).

dependent; that is, in the range of 0.10–1.30 mM, the characteristic signals of  $H_{a,a'}$  and  $H_{b,b'}$  assigned to the piperazinyl moiety shifted upfield 0.15 and 0.27 ppm, respectively, as well as the splitting of CD's H5/H6 protons. These phenomena jointly indicated the tendency of intermolecular association of **1**.

Dynamic light scattering (DLS) measurements were also carried out to investigate the possible self-aggregation of **1** at different concentrations. The result showed that no signal of large assembly could be observed at 0.10 mM, whereas the hydrodynamic diameter of aggregates was increased to 163.3 nm at 2.20 mM, indicating the formation of large-scale aggregation at a higher concentration in aqueous media (Figure 3). Excitingly, the existence of linear aggregates of **1** was also

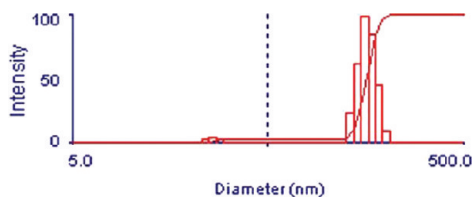


**Figure 3.** Hydrodynamic diameter distributions of **1** (2.20 mM) in aqueous media at  $25^\circ\text{C}$ .

demonstrated by matrix-assisted laser desorption ionization time-of-flight (MALDI-TOF) mass spectrometry, where the peaks at 4812, 6015, 7215, and 8421 were clearly assigned to  $[4\text{M} + \text{H}]^+$ ,  $[5\text{M} + \text{H}]^+$ ,  $[6\text{M} + \text{H}]^+$ , and  $[7\text{M} + \text{H}]^+$ , respectively (Figures 4).

Viscosity measurements were further performed to obtain the rheological properties of supramolecular aggregates in deionized water using an Ubbelohde viscometer at  $25^\circ\text{C}$ . A

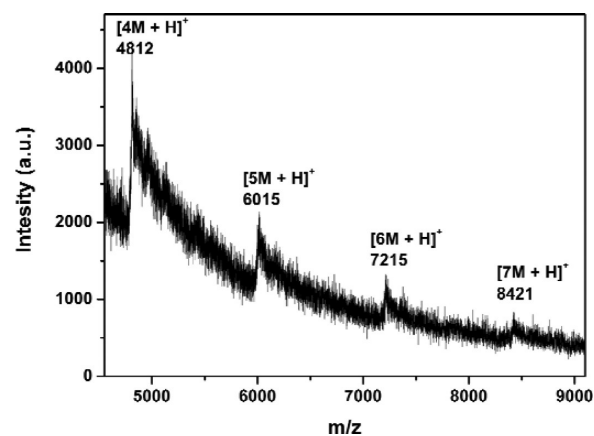


**Figure 4.** MALDI-TOF mass spectrum of compound **1** at 8.60 mM.

plot of specific viscosity versus the monomer concentration of **1** (Figure 5) gave a curve with an obvious change in slope,

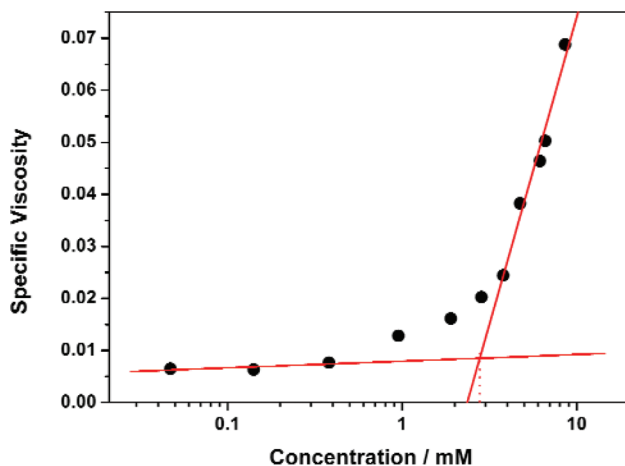
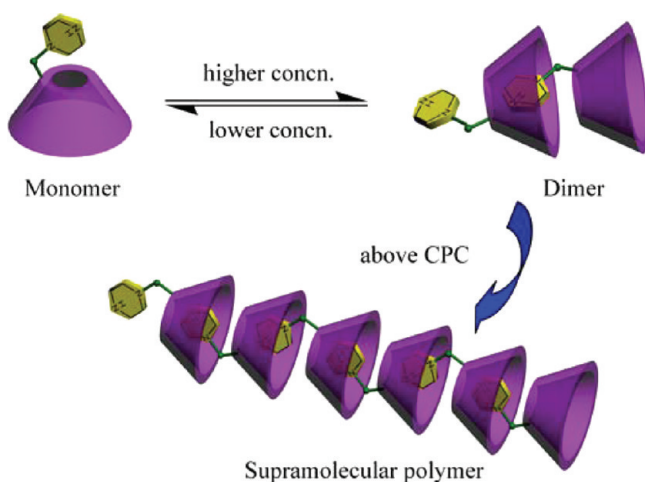


**Figure 5.** Specific viscosity of **1** versus monomer concentration in deionized water at  $25^\circ\text{C}$ .

implementing the supramolecular polymerization process from dimers or oligomers to polymeric species with increasing sizes.<sup>10</sup> Additionally, the lower critical polymerization concentration (CPC) value was found to be 2.68 mM, above which the linear self-aggregates were exclusively formed in aqueous media. Meanwhile, considering that the diffusion coefficient depended on the effective size and shape of a multicomponent species, the diffusion-ordered spectroscopy (DOSY) experiment was carried out to give information about the intermolecular interactions of **1** in aqueous media.<sup>11</sup> When the concentration of monomer **1** increased from 0.10 to 8.60 mM, the measured diffusion coefficients gradually decreased from  $3.53 \times 10^{-10}$  to  $2.25 \times 10^{-10} \text{ m}^2 \cdot \text{s}^{-1}$ , indicative of the concentration-dependent self-aggregation of **1** from monomers to polymers (Figure S7 and S8, Supporting Information). Therefore, we deduced the polymerization process of **1** from monomers to linear supramolecular polymer, as illustrated in Scheme 2.

Subsequently, in order to investigate the binding behaviors of native  $\beta$ -CD with piperazine and dioxane in aqueous solution,  $^1\text{H}$  NMR spectroscopic experiments were performed in  $\text{D}_2\text{O}$  at  $25^\circ\text{C}$ . In the case of dioxane/ $\beta$ -CD complex (**3**), the stoichiometry of host–guest systems was explored by the molar ratio method using  $^1\text{H}$  NMR titration. The curve of

### Scheme 2. Polymerization Process of Monomer 1 To Form Cyclodextrin-Based Supramolecular Polymer in Solution



complex-induced chemical shifts of guest molecules versus molar ratio showed an inflection point at a molar fraction of 1, corresponding to a 1:1 complexation stoichiometry in complex 3 (Figure S9, Supporting Information).<sup>12</sup> After validation of the 1:1 complexation stoichiometry, the thermodynamic parameters of dioxane and CD were measured by the isothermal titration calorimetry (ITC) experiment with reasonable errors as follows:  $\log K_S = 1.45 \pm 0.01$ ,  $\Delta H = -7.02 \pm 0.23 \text{ kJ}\cdot\text{mol}^{-1}$ , and  $T\Delta S = 1.29 \pm 0.19 \text{ kJ}\cdot\text{mol}^{-1}$  (Figure 6 and Figure S10, Supporting Information). These indicated that the complexation of 1,4-dioxane with native  $\beta$ -CD was driven in a thermodynamically favorable way with negative enthalpy and positive entropy change. This result was further confirmed by the  $^1\text{H}$  NMR titration, in which the  $\log K_S$  value was calculated to be 1.32 by analyzing the sequential changes in chemical shift ( $\Delta\delta$ ) of dioxane at varying concentrations of CD using a

nonlinear least-squares curve-fitting method (Figure 7, inset).<sup>13</sup> However, mainly due to the insignificant heat effect and the

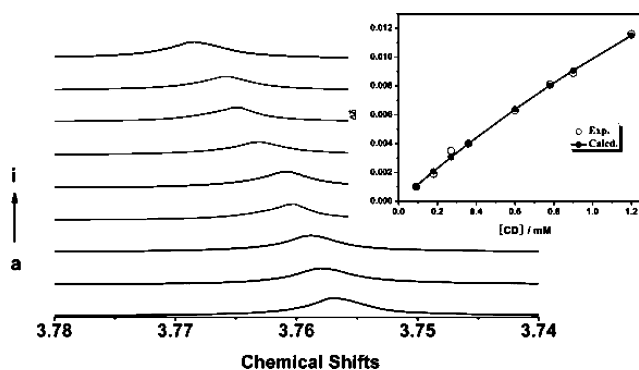


**Figure 7.**  $^1\text{H}$  NMR spectral changes of dioxane upon the addition of  $\beta$ -CD in  $\text{D}_2\text{O}$  at  $25^\circ\text{C}$  ( $[\text{dioxane}] = 1.0 \text{ mM}$ ,  $[\beta\text{-CD}] = 0, 0.9, 1.8, 2.7, 3.6, 6.0, 7.8, 9.0, \text{ and } 12.0 \text{ mM}$  from a to i). Inset: The nonlinear least-squares analysis of the differential chemical shifts ( $\Delta\delta$ ) to calculate the complex formation constant ( $\log K_S$ ) as 1.32.

negligible complexation-induced chemical shifts (Figure S11, Supporting Information), the reliable binding constant of piperazine and CD could not be obtained in our case, indicating the much weaker interaction between piperazine and CD in solution. In comparison to complex 2, it is noteworthy that the extraordinarily strong homodimerization of 1 should be attributed to the effect of supramolecular positive cooperativity, as recently demonstrated for the enhanced binding abilities of  $\alpha$ -CD toward dihexylammonium in the presence of cucurbit[6]uril.<sup>14</sup> Benefiting from the cooperative mutual complexation of the piperazinyl substituent, the mobility of compound 1 was restricted by the hydrogen-bond network of two adjacent  $\beta$ -CDs, and the CD moiety acted as a bulky

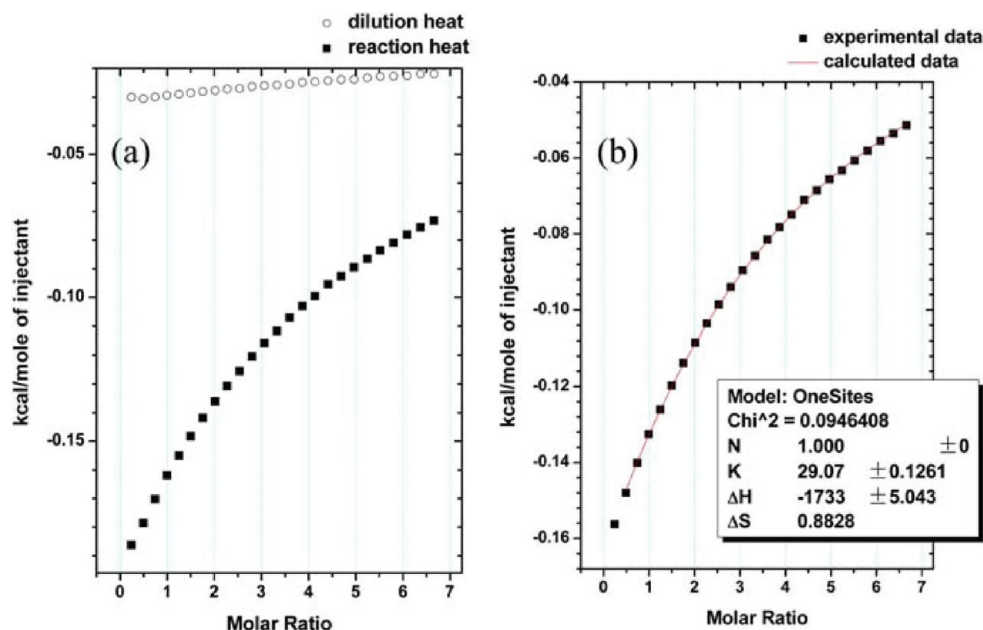


**Figure 6.** Results of the computer simulation of the ITC titration curve upon formation of the dioxane/ $\beta$ -CD complex at  $25^\circ\text{C}$ : (a) heat effects of dilution and of complexation of native  $\beta$ -CD with 1,4-dioxane for each injection during titration of microcalorimetric experiment; (b) “net” heat effect obtained by subtracting the heat of dilution from the heat of reaction, which was analyzed by computer simulation with the use of the “one set of binding sites” model.

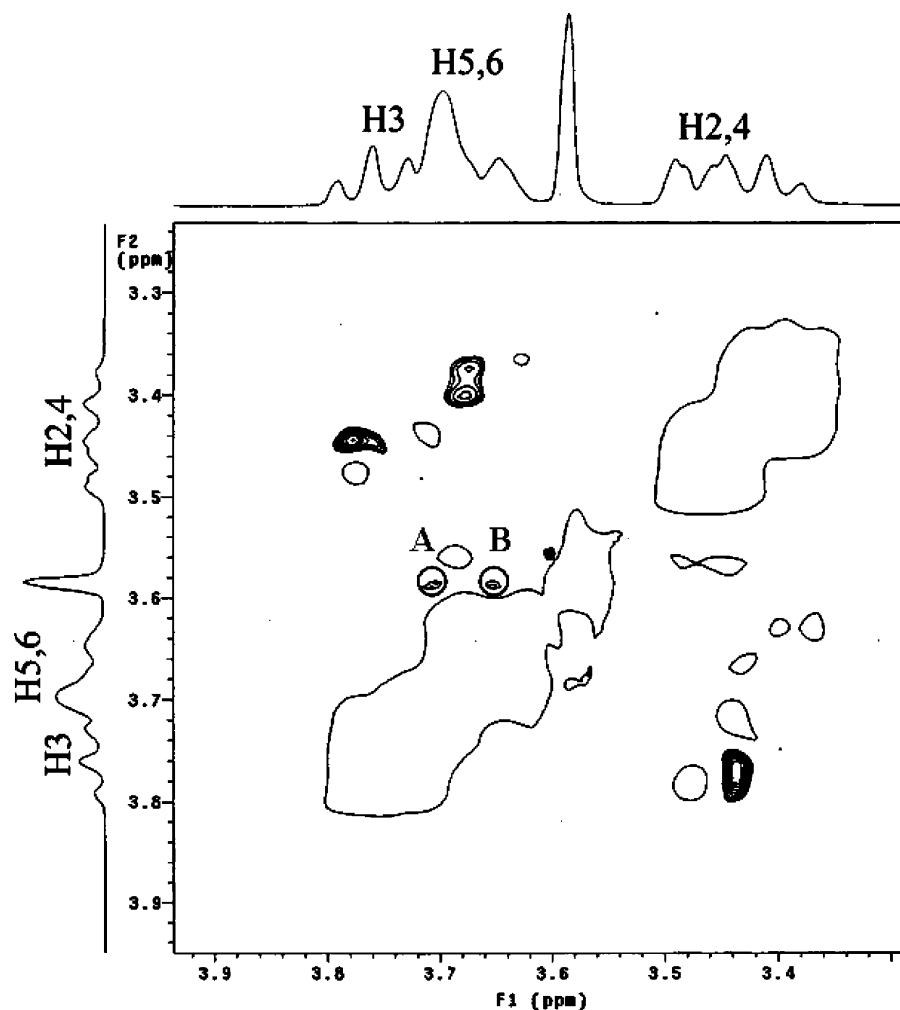


**Figure 8.**  $^1\text{H}$  ROESY spectrum of complex 3 with a mixing time of 270 ms ( $[\text{dioxane}] = 10 \text{ mM}$ ,  $[\text{CD}] = 10 \text{ mM}$ , 300 MHz,  $\text{D}_2\text{O}$ , 25  $^\circ\text{C}$ ).

component surrounding piperazine to increase its rigidity through covalent chemical bonds.

Two-dimensional NMR spectra were employed to investigate the inclusion geometry of CDs with piperazine and 1,4-dioxane in complex 2 and 3. As seen from Figure S12, Supporting Information, the NOE cross-peaks between piperazine and the H3/H5 protons of  $\beta$ -CD (peaks A) were clearly observed in the ROESY spectrum, implying that the guest molecule was shallowly located in the  $\beta$ -CD cavity. Instead, the ROESY spectrum in Figure 8 revealed that the signals of dioxane at 3.58 ppm correlated with H5/H6 protons of  $\beta$ -CD, and no correlation peak was observed between dioxane and H3 protons of  $\beta$ -CD in complex 3, distinctly indicating that dioxane was included at the primary face of  $\beta$ -CD to some extent, as illustrated in Scheme 1. The spatial conformations of complexes 2 and 3 were further confirmed by their crystal structures as describe below.

#### Self-Assembly Behaviors of 1–3 in the Solid State.

More direct evidence for the formation of aggregates was obtained from their crystal structures in the solid state. The single crystals of both piperazine-modified cyclodextrin (1) and piperazine/ $\beta$ -cyclodextrin complex (2) were orthorhombic system with the space group  $P2_12_12_1$ , whereas the single crystal of dioxane/ $\beta$ -CD complex (3) was monoclinic system with the space group  $P2_1$ . As discerned in Figure 9, the CD moieties in crystals 1, 2, and 3 had an approximate 7-fold axis and toroidal

shape, and all of the D-glucose residues were located in the  $^4\text{C}_1$  chair conformation, suggesting that the introduction of substituent group and guest molecules did not dramatically change the original skeleton of native  $\beta$ -CDs.

It is well-documented that monomodified CDs may crystallize in the helical columnar self-assembly, in which the alkyl or aryl substituents intermolecularly penetrate into the hydrophobic cavity of the adjacent  $\beta$ -CD from the secondary face.<sup>15</sup> In the case of the solid-state complex 1, the 1-piperazinyl group attached to the rim of CD stretched straight along the side wall of CD with a 2-fold axis, accompanied by extensive intermolecular hydrogen bonding interactions in the oxygen and nitrogen atoms of two neighboring  $\beta$ -CDs ( $d_{\text{O}3\text{A}\cdots\text{O}2\text{SB}} = 2.781 \text{ \AA}$ ,  $d_{\text{O}23\text{A}\cdots\text{O}4\text{B}} = 3.101 \text{ \AA}$ ,  $d_{\text{O}2\text{A}\cdots\text{O}2\text{SB}} = 3.272 \text{ \AA}$ , and  $d_{\text{N}2\text{A}\cdots\text{O}5\text{B}} = 3.262 \text{ \AA}$ ) to facilitate the formation of the head-to-tail one-dimensional nanoarchitectures (Figure 9a,b). These results were well consistent with the previously reported crystal structures of modified  $\beta$ -CDs tethering with an *N*- or *O*-pivot, because of the flexibility of aliphatic substituents to adjust its conformation through van der Waals forces.<sup>16</sup> Moreover, the X-ray diffractogram of compound 1 displayed a strong peak at  $2\theta = 18.680^\circ$  ( $d = 4.7462 \text{ \AA}$ ,  $I/I_0 = 100$ ), which could be assigned to the characteristic peak of columnar structure of CDs (Figure S13, Supporting Information).<sup>17</sup> Additionally, transmission electron microscopic (TEM) and the scanning electron microscopic (SEM) studies were also carried out to obtain

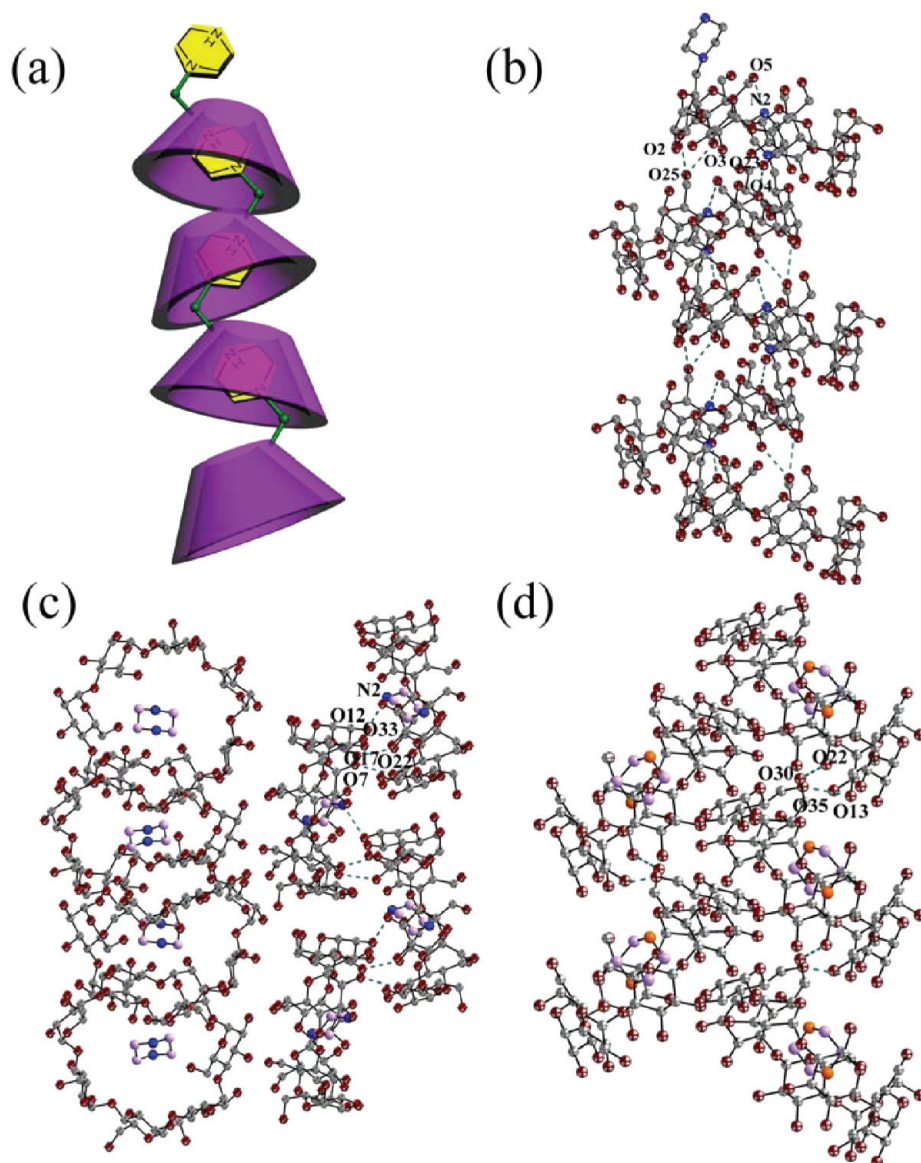


**Figure 9.** (a) Self-assembly mode of **1** and X-ray crystal structures of (b) **1**, (c) **2** with the higher occupation factors (0.670) of guest molecules, and (d) **3**. H atoms and solvent water molecules were omitted for clarity. The nitrogen atoms, oxygen, and carbon atoms in CD are represented as blue, brown, and gray octants, respectively; the carbon, nitrogen, and oxygen atoms in guest molecules are represented as purple, blue, and orange solid spheres, respectively.

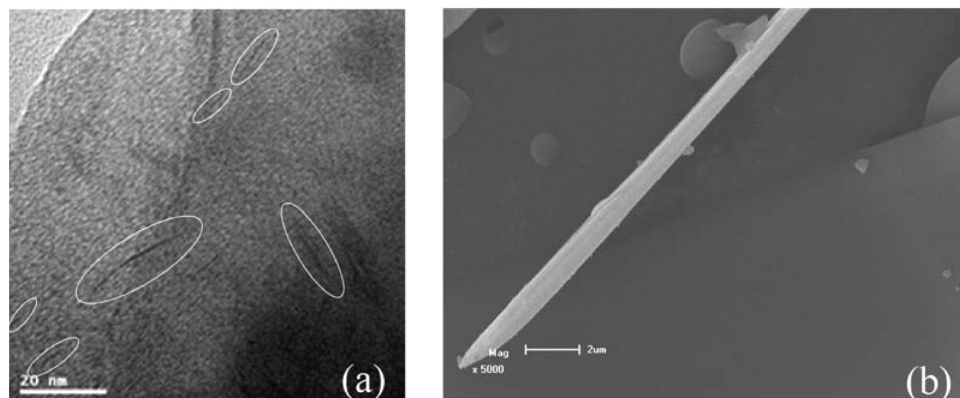


**Figure 10.** Typical (a) TEM and (b) SEM images of the linear supramolecules constructed by compound **1**. The scale bars in TEM and SEM images are 20 nm and 2  $\mu\text{m}$ , respectively.

visual information about the size and shape of the aggregates formed by **1**. The TEM image displayed several linear structures with various lengths of around 20 nm and a similar width of about 1.0 nm (Figure 10a), convincingly indicating highly ordered single-lined structures. Similarly, a fibrous nanowire was also observed in the field of SEM images (Figure 10b), which corresponded to the three-dimensional extension of single lines in TEM images.

Compared with the crystal superstructure of native  $\beta$ -CD containing 6.13 or 7.13 water molecules in the cavity,<sup>18</sup> there was only one water molecule in the unit cell of the 1:1 complex **2**. This extensive desolvation process was mainly due to the hydrophobicity of piperazine to exclude more water molecules from  $\beta$ -CD cavity upon complexation. It should be mentioned herein that, despite the fact that the guest molecules in crystal **2** were disordered over two possible orientations (Figure 10c and Figure S14, Supporting Information) with occupation factors of 0.670 (8) and 0.330 (8), respectively, it did not affect the inclusion modes and aggregation structures. There are three major classes of host–guest complexes produced by native CDs and guest molecules in the solid state: cage-, channel-, and layer-type aggregations through the intermolecular hydrogen-bond network of hydroxyl groups on the primary and secondary faces.<sup>19</sup> However, all of them seemed different from complex **2** to some extent, in which the CD units were located in a staggered pattern with two mutually perpendicular planes along the equatorial direction of the cavities. It is noteworthy that the cooperativity of a H-bonding interaction between a N atom in piperaziny ring and an O atom on the secondary side of  $\beta$ -CD ( $d_{N2A...O12B} = 2.781 \text{ \AA}$ ), multiple hydrogen bonds among the secondary side of two adjacent  $\beta$ -CDs ( $d_{O23A...O7B} = 2.661 \text{ \AA}$ ;  $d_{O33A...O17C} = 2.708 \text{ \AA}$ ), and the hydrophobicity of piperazine jointly fixed the relative orientations and stabilized their geometric configurations in complex **2**. In sharp contrast, the crystallographic complex of piperazine and  $\beta$ -CD was previously prepared with the use of slow solvent evaporation, where each complex consisted of one  $\beta$ -CD, 0.5 piperazine, and 7.2 water molecules in the monoclinic space group  $P2_1$ , and there was no direct host–guest interaction between disordered piperazine molecule and CDs.<sup>20</sup> These results showed that the reaction conditions could profoundly affect the inclusion modes and aggregation structures of CDs. Although **1** and **2** had different aggregation structures in the solid state, they gave the same crystal systems and space groups, which was clearly distinguished from the crystal structure of native  $\beta$ -CD. These results indicated that the introduction of piperazine through either covalent or noncovalent chemical bonds could dramatically change the aggregation structures of CD. Combining the crystallographic results of **1** and **2** together, we reasonably inferred that the hydrogen bonding interaction was a predominant factor to determine the unique aggregation structures of CD derivatives.

Subsequently, the inclusion complex **3** of dioxane and CD was investigated to support this claim. As for the X-ray structure of crystal **3** (Figure 9d), the hydrophobic interaction was the main driving force to encapsulate dioxanes into the cavity of  $\beta$ -CD in a 1:1 ratio, and no hydrogen bonding interaction was observed between the hydroxyl groups of  $\beta$ -CD and dioxane, except the ones formed by the hydroxyl groups of neighboring CDs ( $d_{O22A...O30C} = 2.853 \text{ \AA}$ ;  $d_{O13A...O35C} = 2.781 \text{ \AA}$ ). Due to the loss of effective hydrogen bond network, the aggregation structure of complex **3** was reminiscent of the one of native  $\beta$ -CD, where the CD units maintained a cage-type

packing structure. Through the comparative study of the crystallographic structures of **1–3**, we undoubtedly deduced that hydrogen bonding played a crucial part to govern the superstructure of  $\beta$ -CDs.<sup>21</sup> In crystals **1** and **2**, piperazine acted as a connector to organize the supramolecular aggregation of CDs through noncovalent interactions, whereas the original superstructure of CD was restored in crystal **3**.

## CONCLUSION

In summary, a comparative study of the structurally similar  $\beta$ -CD derivatives **1–3** was fully investigated in aqueous media and the solid state. Compared with the piperazine/ $\beta$ -CD complex **2**, the facile synergetic homodimerization of compound **1** in aqueous solution should be ascribable to the effect of supramolecular positive cooperativity, which was extensively studied in many biological systems. Moreover, the introduction of substituent groups and guest molecules could dramatically change the aggregation structures of  $\beta$ -CDs through the effective hydrogen bonding network in solid state. Therefore, the obtained results in this work afford an alternative way to not only conveniently control the inclusion geometries but also improve our understanding of the bottom-up approach in designing more sophisticated supramolecular materials.

## EXPERIMENTAL SECTION

**Synthesis of Mono-[6-deoxy-6-(1-piperaziny)]- $\beta$ -cyclodextrin (**1**).** A mixture of mono-[6-*O*-(*p*-toluenesulfonyl)]- $\beta$ -CD<sup>22</sup> (1.9 g, 1.5 mmol) and piperazine hexahydrate (3.0 g, 15.4 mmol) was heated at 80 °C under an atmosphere of nitrogen for 8 h. After the mixture cooled to room temperature, the residue was dissolved in a small amount of water, and then washed with 150 mL of acetone at least three times. The crude product was subjected to a column of Sephadex C-25 eluting with 1 M NH<sub>3</sub>·H<sub>2</sub>O and then a silica gel column eluting with CH<sub>3</sub>CN–H<sub>2</sub>O–NH<sub>3</sub>·H<sub>2</sub>O (10:5:3, v/v/v) to give **1** as a white solid in 70% yield ( $R_f = 0.3$ ). Compound **1** was dissolved in hot water to make a saturated solution and then cooled to room temperature. After the insoluble substances were removed by filtration, a small amount of water was added to the filtrate. The resultant solution was kept at room temperature for about 2 weeks, and colorless crystals were obtained available for X-ray crystallographic analysis. <sup>1</sup>H NMR (400 MHz, D<sub>2</sub>O, ppm),  $\delta$  2.46–2.55 (m, 4H), 2.71–2.78 (m, 4H), 3.27–3.96 (m, 42 H, H of C-3, C-5, C-6, C-2, C-4 of  $\beta$ -CD), 4.92–5.00 (m, 7H, H of C-1 of  $\beta$ -CD). <sup>13</sup>C NMR (100 MHz, DMSO-*d*<sub>6</sub>, ppm),  $\delta$  45.4, 54.7, 58.4, 59.8, 72.0, 72.3, 72.4, 72.9, 73.1, 81.3, 81.5, 81.7, 83.9, 101.5, 101.9, 102.0, 102.1. Anal. Calcd for C<sub>46</sub>H<sub>78</sub>N<sub>2</sub>O<sub>34</sub>·8H<sub>2</sub>O: C, 41.01; H, 7.03; N, 2.08. Found: C, 41.10; H, 7.09; N, 2.01. ESI-MS: 1203.5 [M + H]<sup>+</sup>, 1247.1 [M + HCOO]<sup>−</sup>. Crystal data for **1**: C<sub>46</sub>H<sub>106</sub>N<sub>2</sub>O<sub>48</sub>  $M = 1455.33$ , orthorhombic, space group  $P2_12_12_1$ ,  $a = 12.966(10)$ ,  $b = 19.274(14)$ ,  $c = 28.12(2) \text{ \AA}$ ,  $\alpha = 90^\circ$ ,  $\beta = 90^\circ$ ,  $\gamma = 90^\circ$ ,  $V = 7028(9) \text{ \AA}^3$ ,  $F(000) = 3120$ ,  $Z = 4$ ,  $D_c = 1.375 \text{ g}\cdot\text{cm}^{-3}$ ,  $\mu = 0.125 \text{ mm}^{-1}$ , approximate crystal dimensions,  $0.34 \times 0.32 \times 0.20 \text{ mm}^3$ ,  $\theta$  range =  $1.28\text{--}26.00^\circ$ , 51 973 measured reflections of which 13 777 ( $R_{\text{int}} = 0.0516$ ) were unique. final  $R$  indices [ $I > 2\sigma(I)$ ]:  $R_1 = 0.1062$ ,  $wR_2 = 0.3001$ .  $R$  indices (all data):  $R_1 = 0.1211$ ,  $wR_2 = 0.3203$ . Goodness of fit on  $F^2 = 1.213$ .

**Synthesis of Piperazine/ $\beta$ -Cyclodextrin Crystallographic Complex (**2**).** A mixture of  $\beta$ -CD and piperazine hexahydrate in 1:4 molar ratio was dispersed in a small amount of water. Then, the turbid solution was put in a Teflon-lined stainless bomb, which was sealed and then heated at 120 °C under hydrothermal conditions for 2 days. When the solution was cooled to room temperature at the rate of 2 °C/h, the crystals available for X-ray crystallography were obtained. After the crystals were dried under vacuum at 60 °C for 8 h, the target complex was obtained in 65% yield. <sup>1</sup>H NMR (300 MHz, D<sub>2</sub>O, ppm),  $\delta$  2.69 (s, 8H), 3.39–3.84 (m, 42 H, H of C-3, C-5, C-6, C-2, C-4 of  $\beta$ -CD), 4.96 (d, 7H, H of C-1 of  $\beta$ -CD). Anal. Calcd for

$C_{42}H_{70}O_{35} \cdot C_4H_{10}N_2 \cdot 3H_2O$ : C, 43.33; H, 6.80; N, 2.20. Found: C, 43.27; H, 6.86; N, 2.38. Crystal data for **2**:  $C_{46}H_{104}N_2O_{47}$   $M = 1437.31$ , orthorhombic, space group  $P2_12_12_1$ ,  $a = 14.9066(5)$ ,  $b = 20.4267(8)$ ,  $c = 21.8526(9)$  Å,  $\alpha = 90^\circ$ ,  $\beta = 90^\circ$ ,  $\gamma = 90^\circ$ ,  $V = 6654.0(4)$  Å<sup>3</sup>,  $F(000) = 3080$ ,  $Z = 4$ ,  $D_c = 1.435$  g·cm<sup>-3</sup>,  $\mu = 0.130$  mm<sup>-1</sup>, approximate crystal dimensions,  $0.16 \times 0.14 \times 0.14$  mm<sup>3</sup>,  $\theta$  range =  $1.36$ – $26.00^\circ$ , 54 957 measured reflections of which 7165 ( $R_{int} = 0.0611$ ) were unique. Final  $R$  indices [ $I > 2\sigma(I)$ ]:  $R_1 = 0.0585$ ,  $wR_2 = 0.1428$ .  $R$  indices (all data):  $R_1 = 0.0601$ ,  $wR_2 = 0.1472$ . Goodness of fit on  $F^2 = 1.185$ .

**Synthesis of Dioxane/ $\beta$ -Cyclodextrin Crystallographic Complex (3).** Inclusion complex **3** was prepared from the mixture of  $\beta$ -CD and 1,4-dioxane following the similar procedure as described above for **2** and was isolated in 70% yield. <sup>1</sup>H NMR (300 MHz, D<sub>2</sub>O, ppm),  $\delta$  3.40–3.90 (m, 50 H, H of dioxane and C-3, C-5, C-6, C-2, C-4 of  $\beta$ -CD), 4.95 (d, 7H, H of C-1 of  $\beta$ -CD). Anal. Calcd for  $C_{42}H_{70}O_{35} \cdot C_4H_8O_2 \cdot 5H_2O$ : C, 42.07; H, 6.75. Found: C, 42.20; H, 6.80. Crystal data for **3**:  $C_{46}H_{92}O_{44}$   $M = 1349.20$ , monoclinic, space group  $P2_1$ ,  $a = 15.274(12)$ ,  $b = 10.178(8)$ ,  $c = 20.961(16)$  Å,  $\alpha = 90^\circ$ ,  $\beta = 110.251(7)^\circ$ ,  $\gamma = 90^\circ$ ,  $V = 3057(4)$  Å<sup>3</sup>,  $F(000) = 1440$ ,  $Z = 2$ ,  $D_c = 1.466$  g·cm<sup>-3</sup>,  $\mu = 0.132$  mm<sup>-1</sup>, approximate crystal dimensions,  $0.34 \times 0.32 \times 0.28$  mm<sup>3</sup>,  $\theta$  range =  $1.42$ – $25.00^\circ$ , 20 495 measured reflections of which 10 151 ( $R_{int} = 0.1371$ ) were unique. Final  $R$  indices [ $I > 2\sigma(I)$ ]:  $R_1 = 0.1010$ ,  $wR_2 = 0.2666$ .  $R$  indices (all data):  $R_1 = 0.1127$ ,  $wR_2 = 0.2839$ . Goodness of fit on  $F^2 = 1.037$ .

## ■ ASSOCIATED CONTENT

### Supporting Information

X-ray crystallographic data in CIF format (CCDC no. 680226 for **1**, CCDC no. 680224 for **2**, and CCDC no. 827901 for **3**), general experimental procedures, characterization data for compound **1**–**3**, ROESY, DOSY, and XRD spectra of **1**, <sup>1</sup>H NMR titration of complexes **2** and **3**, microcalorimetric titration of 1,4-dioxane/ $\beta$ -CD system, and ROESY spectrum of **2**. This material is available free of charge via the Internet at <http://pubs.acs.org>.

## ■ AUTHOR INFORMATION

### Corresponding Author

\*E-mail: [yuliu@nankai.edu.cn](mailto:yuliu@nankai.edu.cn).

## ■ ACKNOWLEDGMENTS

We thank the 973 Program (Grant 2011CB932502), NNSFC (Grant Nos. 20932004 and 91027007), and the Fundamental Research Funds for the Central Universities for the financial support (Grant BE018201).

## ■ REFERENCES

- (1) (a) Bellia, F.; La Mendola, D.; Pedone, C.; Rizzarelli, E.; Savianoc, M.; Vecchia, G. *Chem. Soc. Rev.* **2009**, *38*, 2756–2781. (b) Harada, A.; Hashidzume, A.; Yamaguchi, H.; Takashima, Y. *Chem. Rev.* **2009**, *109*, 5974–6023. (c) Brovelli, S.; Cacialli, F. *Small* **2010**, *6*, 2796–2820. (d) Chen, G.; Jiang, M. *Chem. Soc. Rev.* **2011**, *40*, 2254–2266.
- (2) (a) Rekharsky, M. V.; Inoue, Y. *Chem. Rev.* **1998**, *98*, 1875–1918. (b) Brewster, M. E.; Loftsson, T. *Adv. Drug Delivery Rev.* **2007**, *59*, 645–666.
- (3) (a) Clark, J. L.; Stezowski, J. J. *J. Am. Chem. Soc.* **2001**, *123*, 9880–9888. (b) Liu, Y.; Zhao, Y.-L.; Zhang, H.-Y.; Song, H.-B. *Angew. Chem., Int. Ed.* **2003**, *42*, 3260–3263. (c) Caira, M. R.; de Vries, E. J. C.; Nassimbeni, L. R. *Chem. Commun.* **2003**, 2058–2059. (d) Onagi, H.; Blake, C. J.; Easton, C. J.; Lincoln, S. F. *Chem.—Eur. J.* **2003**, *9*, 5978–5988. (e) Terao, J.; Tang, A.; Michels, J. J.; Krivokapic, A.; Anderson, H. L. *Chem. Commun.* **2004**, 56–57.
- (4) Chen, Y.; Zhang, Y.-M.; Liu, Y. *Chem. Commun.* **2010**, 5622–5633.

(5) (a) Coulston, R. J.; Onagi, H.; Lincoln, S. F.; Easton, C. J. *J. Am. Chem. Soc.* **2006**, *128*, 14750–14751. (b) Terao, J.; Ikai, K.; Kambe, N.; Seki, S.; Saeki, A.; Ohkoshi, K.; Fujihara, T.; Tsujia, Y. *Chem. Commun.* **2011**, 6816–6818.

(6) Lincoln, S. F.; Coates, J. H.; Easton, C. J.; Van Eyk, S. J.; May, B. L.; Singh, P.; Williams, M. L.; Stile, M. A. PCT Int. Appl. WO 90/02141, 1990.

(7) (a) Yamauchi, K.; Takashima, Y.; Hashidzume, A.; Yamaguchi, H.; Harada, A. *J. Am. Chem. Soc.* **2008**, *130*, 5024–5025. (b) Harada, A.; Takashima, Y.; Yamaguchi, H. *Chem. Soc. Rev.* **2009**, *38*, 875–882.

(8) Liu, Y.; Yang, Z.-X.; Chen, Y. *J. Org. Chem.* **2008**, *73*, 5298–5304.

(9) (a) Park, J. W.; Song, H. E.; Lee, S. Y. *J. Phys. Chem. B* **2002**, *106*, 5177–5183. (b) Park, J. W.; Song, H. E.; Lee, S. Y. *J. Phys. Chem. B* **2002**, *106*, 7186–7192.

(10) Dong, S.; Luo, Y.; Yan, X.; Zheng, B.; Ding, X.; Yu, Y.; Ma, Z.; Zhao, Q.; Huang, F. *Angew. Chem., Int. Ed.* **2011**, *50*, 1905–1909.

(11) Cohen, Y.; Avram, L.; Frish, L. *Angew. Chem., Int. Ed.* **2005**, *44*, 520–554.

(12) Liu, Y.; Zhang, N.; Chen, Y.; Wang, L.-H. *Org. Lett.* **2007**, *9*, 315–318.

(13) García-Río, L.; Hervés, P.; Leis, J. R.; Mejuto, J. C.; Pérez-Juste, J.; Rodríguez-Dafonte, P. *Org. Biomol. Chem.* **2006**, *4*, 1038–1048.

(14) Rekharsky, M. V.; Yamamura, H.; Kawai, M.; Osaka, I.; Arakawa, R.; Sato, A.; Ko, Y. H.; Selvapalam, N.; Kim, K.; Inoue, Y. *Org. Lett.* **2006**, *8*, 815–818.

(15) (a) Harata, K.; Takenaka, Y.; Yoshida, N. *J. Chem. Soc., Perkin Trans.* **2001**, *2*, 1667–1673. (b) Liu, Y.; You, C.-C.; Zhang, M.; Weng, L.-H.; Wada, T.; Inoue, Y. *Org. Lett.* **2000**, *2*, 2761–2763.

(16) Liu, Y.; Fan, Z.; Zhang, H.-Y.; Yang, Y.-W.; Ding, F.; Liu, S.-X.; Wu, X.; Wada, T.; Inoue, Y. *J. Org. Chem.* **2003**, *68*, 8345–8352.

(17) (a) Harding, M. M.; MacLennan, J. M.; Paton, R. M. *Nature* **1978**, *274*, 612–615. (b) Liu, Y.; Wang, H.; Chen, Y.; Ke, C.-F.; Liu, M. *J. Am. Chem. Soc.* **2005**, *127*, 657–666.

(18) (a) Lindner, K.; Saenger, W. *Carbohydr. Res.* **1982**, *99*, 103–115. (b) Betzel, C.; Saenger, W.; Hingerty, B. E.; Brown, G. M. *J. Am. Chem. Soc.* **1984**, *106*, 7545–7557.

(19) (a) Harata, K. *Chem. Rev.* **1998**, *98*, 1803–1827. (b) Lindner, H. J.; Yuan, D.-Q.; Fujita, K.; Kubo, K.; Lichtenthaler, F. W. *Chem. Commun.* **2003**, 1730–1731.

(20) Areea, T.; Chaichitb, N. *Supramol. Chem.* **2009**, *21*, 384–393.

(21) Zhao, Y.-L.; Benitez, D.; Yoon, I.; Stoddart, J. F. *Chem.—Asian J.* **2009**, *4*, 446–456.

(22) Petter, R. C.; Salek, J. S.; Sikorski, C. T.; Kumaravel, G.; Lin, F. *T. J. Am. Chem. Soc.* **1990**, *112*, 3860–3868.